Using Linear Interpolation to Reduce the Training Samples for Regression Based Visible Light Positioning System
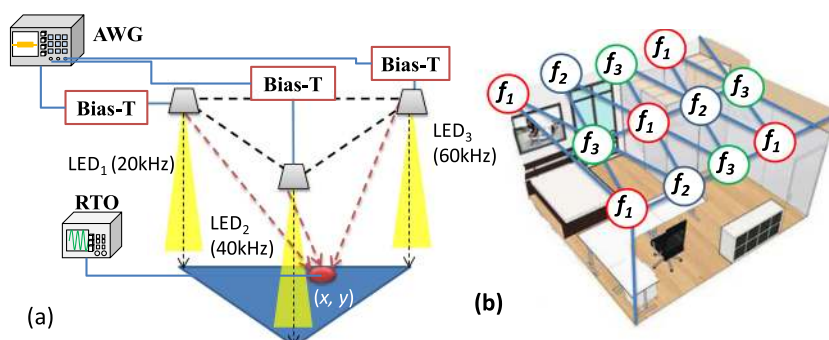
Yu-Chun Wu
Ke-Ling Hsu
Yang Liu
Chong-You Hong
Chi-Wai Chow
Chien-Hung Yeh
Xin-Lan Liao
Kun-Hsien Lin
Yi-Yuan Chen

Using Linear Interpolation to Reduce the Training Samples for Regression Based Visible Light Positioning System

Yu-Chun Wu,[1] **Ke-Ling Hsu,**[1] **Yang Liu,**[2] **Chong-You Hong,**[1]
Chi-Wai Chow [ID]**,**[1] **Chien-Hung Yeh** [ID]**,**[3] **Xin-Lan Liao,**[4]
Kun-Hsien Lin,[4] **and Yi-Yuan Chen**[4]

[1]Department of Photonics, College of Electrical and Computer Engineering, National Chiao
Tung University, Hsinchu 30010, Taiwan
[2]Philips Electronics Ltd., Shatin, Hong Kong
[3]Department of Photonics, Feng Chia University, Taichung 40724, Taiwan
[4]Industrial Technology Research Institute, Hsinchu 31040, Taiwan

Abstract: We put forward and experimentally demonstrate a second order machine-learning (ML) based visible-light-positioning (VLP) system using simple linear interpolation algorithm to reduce the training samples required in the ML algorithm. Algorithms of the second order regression ML model using 2,430 training samples; and using the reduced training samples of 570 with and without the proposed linear interpolation are compared and discussed. We can observe that the positioning accuracy of using training samples of 570 with the proposed interpolation can have similar performance when compared with using 2,430 training samples. The training samples are reduced by ∼76.5%. Here, off-the-shelf LED lamps and low bandwidth electrical and optical components are employed; and the system is cost-effective. Good quality on-off keying (OOK) identifier (ID) signals are retrieved after frequency down-conversion from 20 kHz, 40 kHz and 60 kHz without and with optical background noises respectively.

Index Terms: Light emitting diode (LED), visible light communication (VLC), visible light positioning (VLP).

1. Introduction

The Global Positioning System (GPS) is well established and commonly used nowadays for outdoor. As GPS relies on the communications with the satellites and mobile network base stations, the performance of GPS will significantly reduce in indoor or underground areas. Recently, the traditional lighting devices, such as fluorescent lamps, are gradually replaced by solid-state lighting devices, such as light-emitting-diodes (LEDs). As the solid-state lighting can be switched on and off at a relatively high speed, it can be used to provide both illumination and communication, which is known as visible light communication (VLC) [1]–[8]. Using the existing LED lighting infrastructure can also provide visible light positioning (VLP). Similar to GPS, VLP can provide the navigation information to find the target indoor destinations. It can be used for asset tracking in hospitals or
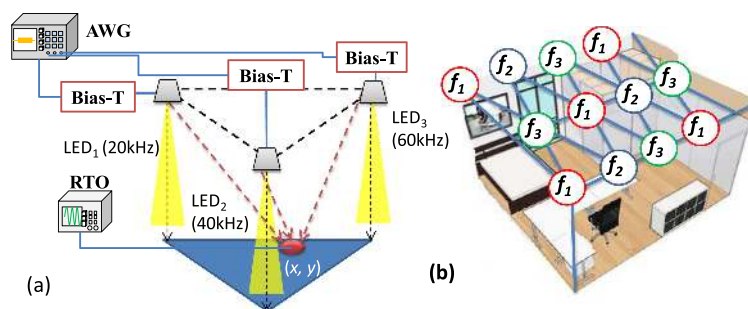
Fig. 1. (a) Experimental setup of the ML based VLP. (b) Unit cells can be repeated to cover indoor environment.

universities. It can also be used to provide location-aware services, such as antique information in museums or item prices in shopping malls. One simple VLP scheme is based on visible light identifier (ID) [9], in which unique ID is emitted by different lamps. However, the accuracy is limited by the lighting zone. Proximity based VLP is demonstrated [10]; however, this scheme requires to decode the rolling-shutter patterns of the camera image sensor. Angle-of-arrival (AOA) based VLP is also proposed, and no synchronization is needed between the LED transmitter (Tx) with receiver (Rx); however, these schemes either require an accelerometer at the Rx [11] or multiple Rxs, such as quadrature photodiode (QPD) [12]. Time-of-arrival (TOA) and time-difference-of-arrival (TDOA) based VLP are proposed [13]; however exact arrival time and synchronization between the Tx and Rx are required. Received signal strength (RSS) based VLP are proposed [14], [15], in which the Rx power increases when the distance between Tx and Rx decreases. Recently, an RSS based VLP using machine learning (ML) to increase the positioning accuracy is demonstrated [16]. However, a large number of training samples are required in the ML training process to achieve high positioning accuracy.

In this work, we put forward and experimentally demonstrate a ML based VLP system using simple linear interpolation algorithm to reduce the training samples required in the ML algorithm. Algorithms of the second order regression ML model using many training samples; and using reduced training samples with and without the proposed linear interpolation are compared and discussed. We can observe that the positioning accuracy of using training samples of 570 with the proposed interpolation can have similar performance when compared with using 2,430 training samples. The training samples are reduced by ∼76.5%. Here, off-the-shelf LED lamps and low bandwidth electrical and optical components are employed; and the system is cost-effective.

2. Algorithms and Experiment

Fig. 1(a) shows the experimental setup of the ML based VLP. Here, three unique IDs in on-off keying (OOK) modulation format with three carrier frequencies (f_1, f_2, f_3) are used to modulate the LED; and the Rx is at location (x, y) inside the unit cell. The received luminance by the Rx at 360 lux in the experiment. The LED is commercially available. It has an power consumption of 5 W using 12 V bias voltage. It has an emitting angle of 28°. An arbitrary wavelength generator (AWG, Tektronix AFG3252C) provides the 20 kHz, 40 kHz and 60 kHz frequency up-converted 10 kbit/s OOK signals to the LEDS. The AWG has bandwidth and sample rate of 240 MHz and 2MSample/s respectively. The Rx is a silicon based detector (Thorlab PDA36A-EC). It consists of a silicon PIN photodiode (PD) with a transimpedance amplifier. The PD has the detection area of 3.6 × 3.6 mm and wavelength range from 350 nm to 1100 nm. The responsivity of the PD is 0.65 A/W and the detection bandwidth of 10 MHz. The Rx is attached to a real-time oscilloscope (RTO, Tektronix MDO3024) for signal analysis. it has bandwidth and sample rate of 200 MHz and 2.5 GSample/s respectively. In the experiment, two measurement conditions are employed to emulate the VLP conditions without and with optical background noises. The background noises are launched by
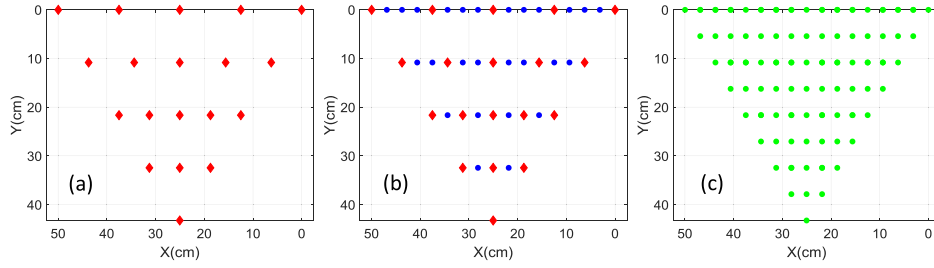
Fig. 2. Training locations inside the unit cell. (a) Red diamond: 19 training locations; (b) blue circle: Interpolated locations; (c) green circle: 81 training locations.

the compact fluorescent lamps (CFLs) present in the laboratory. When the CFLs are turn-off to emulate the no optical background noises scenario, the luminance inside the unit cell is about 360 lux. When the CFLs are turn-on to emulate the existence of optical background noises, the luminance is about 450 lux. Fig. 1(b) illustrates that these unit cells can be repeated to cover the entire indoor environment. Since each LED in the entire indoor environment has an unique ID, in practical implementation, the location of unit cell will be identified first. Then, the position of the Rx inside this particular unit cell will be estimated.

Fig. 2(a)–(c) show the training locations inside the unit cell. In the first experiment, we employ 19 training locations indicated as red diamonds as shown in Fig. 2(a). The RSS data at each training location (i.e., x-and y-coordinates) are measured 30 times; hence there are total 570 training samples in the reduced sample case. In the second experiment, the 19 training locations are interpolated to produce a total 45 locations points via interpolation algorithm, which are indicated as blue circles as shown in Fig. 2(b). In the third experiment, 81 training locations are used to train the second order regression ML model. They are marked in green circles as shown in Fig. 2(c); hence there are a total 2,430 training samples.

The linear interpolation model is shown in Eq. (1), where d_1 and d_2 are distance between the interpolated location and the adjacent location respectively. $p_{i,1}$ and $p_{i,2}$ are the received intensity of each LEDs of two adjacent locations, where $i = 1, 2, 3$. $p_{i,n}$ is each LED calculated intensity at the interpolated location.

$$p_{i,n} = \frac{d_1\,p_{i,1} + d_2\,p_{i,2}}{d_1 + d_2} \tag{1}$$

After obtaining the locations and the intensity of the 570 training samples. The second order regression ML model is applied is shown in Eq. (2), where $\mathbf{W}$, Φ and t are the weight, amplitude and target vectors respectively. p_i and p_j are received intensity of each LEDs. D is the dimension, as there are three LEDs in this experiment, D equals three.

$$\hat{f} = w^{(0)} + \sum_{i=1}^{D} w^{(i)} p_i + \sum_{i=1}^{D} \sum_{j=1}^{D} w^{(i,j)} p_i p_j = \Phi W_{ML} \tag{2}$$

Eq. (2) can be decomposed into the x- and y-coordinates, as shown in Eq. (3).

$$\begin{cases} f_x = w_x^{(0)} + w_x^{(1)} p_1 + w_x^{(2)} p_2 + w_x^{(3)} p_3 + w_x^{(11)} p_1{}^2 + \cdots + w_x^{(22)} p_2{}^2 + w_x^{(23)} p_2 p_3 + w_x^{(33)} p_3{}^2 \\ f_y = w_y^{(0)} + w_y^{(1)} p_1 + w_y^{(2)} p_2 + w_y^{(3)} p_3 + w_y^{(11)} p_1{}^2 + \cdots + w_y^{(22)} p_2{}^2 + w_y^{(23)} p_2 p_3 + w_y^{(33)} p_3{}^2 \end{cases} \tag{3}$$

3. Results and Discussions

Figs. 3(a) and (b) show the measured cumulative distribution function (CDF) at different position errors without and with the optical background noises respectively. In each environment, the CDF of using the reduced training sample case without (i.e., 19 training locations) and with the proposed
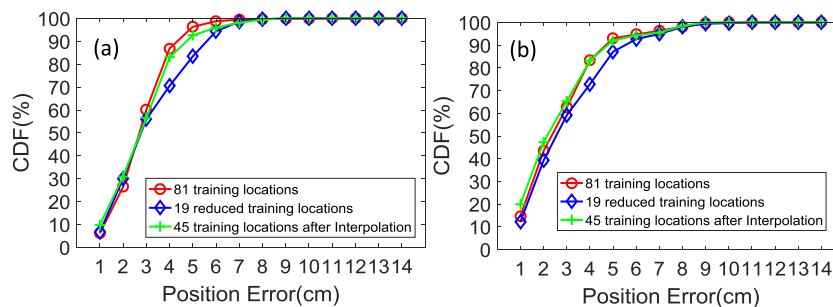
Fig. 3. Experimental CDF against the position errors (a) without and (b) with the optical background noises.

(a) 20 kHz no background   **(b) 20 kHz with background**   **(c) 40 kHz no background**   **(d) 40 kHz with background**   **(e) 60 kHz no background**   **(f) 60 kHz with background**
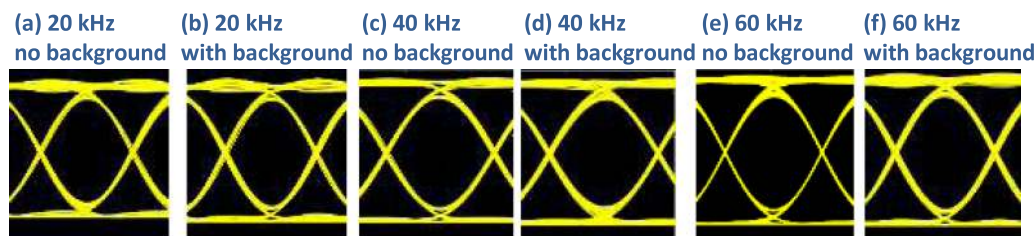

Fig. 4. Experimental OOK ID signals without and with the optical background noises.

linear interpolation (i.e., 45 training locations), as well as using 81 training locations are compared. We can observe that the influence by the background optical noises is small. For example, when using 81 training locations, about 98% of testing samples have position error $\leqq$ 6 cm and about 100% have position error $\leqq$ 8 cm without background noises. When background noises are present, about 95% of testing samples have position error $\leqq$ 6 cm and about 100% have position error $\leqq$ 9 cm. The small influence of the optical background noises is because the VLP signals are frequency up-converted. As shown in Fig. 3(a), we can also observe that the CDF is 87% at position error within 4 cm when using 81 training locations; and the CDF reduces to 70% when using 19 training locations. By using the proposed interpolation to 45 training locations, the CDF restores to 83%. This means that the CDF only decreases by 4.6% at position error within 4 cm while the required number of training samples are reduced by 76.5% when the proposed interpolation is employed. When the optical background noises are present as illustrated in Fig. 3(b), the CDF is 83% at position error within 4 cm when using 81 training locations; and the CDF reduces to 73% when using 19 training locations. By using the proposed interpolation to 45 training locations, the CDF restores to 83%. In this demonstration, we define 19 training locations as shown in Fig. 2(a). By defining more training locations inside an unit cell, the VLP accuracy could be improved. Besides, we use the simple second order regression model. Using more advanced ML models may also improve the accuracy.

Figs. 4(a)–(f) illustrates the measured 10 kbit/s OOK ID signals after frequency down-conversion from 20 kHz, 40 kHz, 60 kHz without and with the optical background noises respectively. We can observe that the received ID signals are clear; and the measured Q(dB) values for the 20 kHz, 40 kHz and 60 kHz without optical background noises are 13.2 dB, 12.8 dB and 12.4 dB respectively; and that with the optical background noises are 12.7 dB, 13.2 dB and 12.7 dB respectively.

4. Conclusion

We put forward and demonstrated a ML based VLP system using simple linear interpolation algorithm to reduce the training samples required in the ML algorithm. We can observe that the

positioning accuracy of using training samples of 570 with the proposed interpolation can have similar performance when compared with using 2,430 training samples. For example, the CDF only decreased by 4.6% at position error within 4 cm while the required number of training samples were reduced by 76.5% when the proposed interpolation was employed. Besides, good quality OOK ID signals were retrieved after frequency down-conversion from 20 kHz, 40 kHz and 60 kHz under different environment conditions.

References

[1] H. L. Minh *et al.*, "100-Mb/s NRZ visible light communications using a post-equalized white LED," *IEEE Photon. Technol. Lett.*, vol. 21, no. 15, pp. 1063–1065, Aug. 2009.

[2] J. Vučić, C. Kottke, S. Nerreter, K. D. Langer, and J. W. Walewski, "513 Mbit/s visible light communications link based on DMT-modulation of a white LED," *J. Lightw. Technol.*, vol. 28, no. 24, pp. 3512–3518, Dec. 2010.

[3] Z. Wang, C. Yu, W. D. Zhong, J. Chen, and W. Chen, "Performance of a novel LED lamp arrangement to reduce SNR fluctuation for multi-user visible light communication systems," *Opt. Express*, vol. 20, pp. 4564–4573, 2012.

[4] H. H. Lu, Y. P. Lin, P. Y. Wu, C. Y. Chen, M. C. Chen, and T. W. Jhang, "A multiple-input-multiple-output visible light communication system based on VCSELs and spatial light modulators," *Opt. Express*, vol. 22, pp. 3468–3474, 2014.

[5] B. Janjua *et al.*, "Going beyond 4 Gbps data rate by employing RGB laser diodes for visible light communication," *Opt. Express*, vol. 23, pp. 18746–18753, 2015.

[6] H. Chun *et al.*, "LED based wavelength division multiplexed 10 Gb/s visible light communications," *J. Lightw. Technol.*, vol. 34, no. 13, pp. 3047–3052, Jul. 2016.

[7] Y. F. Liu, C. H. Yeh, and C. W. Chow, "Alternating-signal-biased system design and demonstration for visible light communication," *IEEE Photon. J.*, vol. 5, no. 4, Aug. 2013, Art. no. 7901806.

[8] C. Hsu, C. Chow, I. Lu, Y. Liu, C. Yeh, and Y. Liu, "High speed imaging 3 × 3 MIMO phosphor white-light LED based visible light communication system," *IEEE Photon. J.*, vol. 8, no. 6, Dec. 2016, Art. no. 7907406.

[9] S. Ayub, S. Kariyawasam, M. Honary, and B. Honary, "Visible light ID system for indoor localization," *Proc. IET Int. Conf. Wireless, Mobile Multimedia Netw.*, 2013, pp. 254–257.

[10] C. Y. Xie, W. P. Guan, Y. X. Wu, L. T. Fang, and Y. Cai, "The LED-ID detection and recognition method based on visible light positioning using proximity method," *IEEE Photon. J.*, vol. 10, no. 2, Apr. 2018, Art. no. 7902116.

[11] M. Yasir, S. W. Ho, and B. N. Vellambi, "Indoor positioning system using visible light and accelerometer," *J. Lightw. Technol.*, vol. 32, no. 19, pp. 3306–3316, Oct. 2014.

[12] S. Cincotta, C. W. He, A. Neild, and J. Armstrong, "High angular resolution visible light positioning using a quadrant photodiode angular diversity aperture receiver," *Opt. Express*, vol. 26, pp. 9230–9242, 2018.

[13] P. F. Du, S. Zhang, C. Chen, A. Alphones, and W. D. Zhong, "Demonstration of a low-complexity indoor visible light positioning system using an enhanced TDOA scheme," *IEEE Photon. J.*, vol. 10, no. 4, Aug. 2018, Art. no. 7905110.

[14] N. Chaudhary, L. N. Alves, and Z. Ghassemlooy, "Current trends on visible light positioning techniques," in *Proc. 2nd West Asian Colloq. Opt. Wireless Commun.*, 2019, pp. 100–105.

[15] C. W. Hsu *et al.*, "Visible light positioning and lighting based on identity positioning and RF carrier allocation technique using a solar cell receiver," *IEEE Photon. J.* vol. 8, no. 4, Aug. 2016, Art. no. 7905507.

[16] Y. C. Chuang, Z. Q. Li, C. W. Hsu, Y. Liu, and C. W. Chow, "Visible light communication and positioning using positioning cells and machine learning algorithms," *Opt. Express*, vol. 27, pp. 16377–16383, 2019.